

# Building a 3.3 - 3.8 GHz 802.16a WiMAX LNA on FR4 Material



## White Paper

By: Lu, Xiao

### Introduction

This article presents the design of a 3.3 - 3.8 GHz LNA suitable for IEEE 802.16a WiMAX customer premise equipment (CPE) and base transceiver stations (BTS), built on inexpensive FR4 copper laminate epoxy glass board material using the Avago Technologies ATF-54143 E-pHEMT (enhancement-mode pseudomorphic high electron mobility transistor).

The high loss tangent ( $\delta$ ) and relatively variable dielectric constant ( $\epsilon_r$ ) of grade FR4 copper laminate epoxy glass material ( $\delta = 0.04$ ,  $\epsilon_r = 4.6$ ) generally limits its use to applications below 3 GHz. For higher frequencies, designers usually use more expensive materials such as Rogers RO4350B glass-reinforced hydrocarbon/ceramic laminate [2] with  $\delta = 0.003$  and  $\epsilon_r = 3.48$ . With the booming of WiMAX as a substitute for the existing broadband wireline infrastructure in the last mile, people are now designing and testing WiMAX customer premise equipment (CPE) and base transceiver stations (BTS) operating at around 3.5 GHz. Properly designed circuits on FR4 board can help reduce the transceiver cost. Based on theoretical analysis and ADS simulation, this paper presents a successful WiMAX LNA built on FR4 board using the Avago ATF-54143 E-pHEMT.

### Target Analysis

With a single 3.6 V supply, this E-pHEMT LNA delivers measured 0.82 dB noise figure (NF), 12.8 dB gain, +19 dBm output power at 1 dB gain compression ( $OP_{1dB}$ ), 36.7 dBm third-order output intercept point ( $OIP_3$ ), -20 dB input return loss (IRL) and -12 dB output return loss (ORL) at 3.5 GHz.

To arrive at a balance between noise figure, gain and linearity, the device drain source current ( $I_{ds}$ ) was chosen to be 60 mA with a 3V drain to source voltage, and thus the gate to source voltage was 0.59V. According to the data sheet [3] of the ATF-54143, this E-pHEMT transistor has the following typical features at 3.5 GHz:  $F_{min} = 0.65$  dB,  $G_a = 14.5$  dB,  $OIP_3 = +37.2$  dBm, and  $S_{11} = 0.608 \angle 149.6^\circ$  ( $VSWR \approx 4.1$ ), and  $\Gamma_{opt} = 0.32 \angle -170^\circ$ .

The circuit can be simulated in both linear and nonlinear operation modes by using the EEs of Advanced Design System (ADS) software. A two-port S-parameter file in the Touchstone format was used to simulate the gain, noise figure and input/output return loss; an ADS model based on the data sheet [3] was applied to simulate the bias conditions and linearity.

Accurate equivalent models for the resistors, inductors, capacitors and microstrip lines are critical for exact simulation because they dominate board circuit tuning. Thus, device models from Murata or Toko products are adopted to model the capacitors and inductors from these two vendors, and board features provided by the FR4 vendor are adopted to model the microstrip lines. Figure 1(a) shows the schematic of the circuit, and Figure 1(b) is the correspondent ADS simulation file that includes all the models.

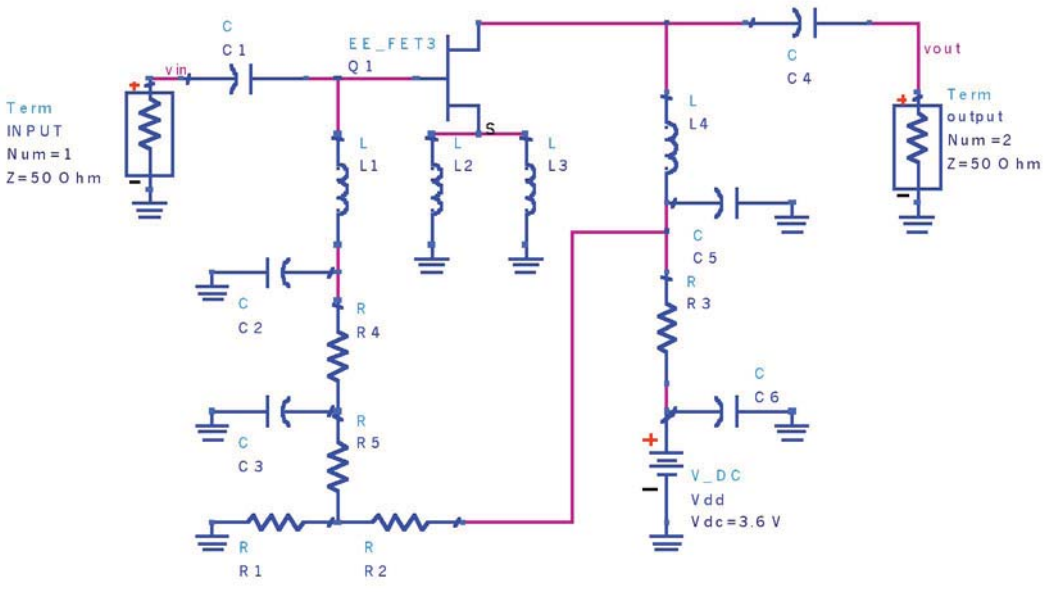


Figure 1(a). ATF-54143 LNA circuit schematic

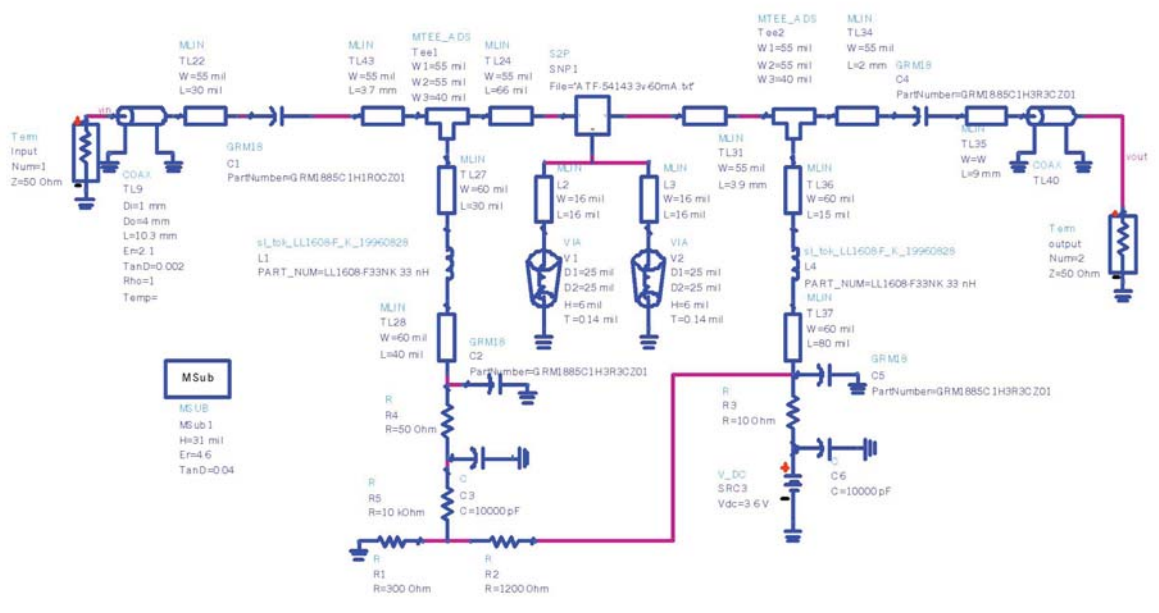


Figure 1(b). Corresponding ADS simulation for Figure 1(a)

## RF Input Matching

RF input matching always plays a key role in an LNA design. It is not only a way to achieve a low NF, it's also the way to obtain higher IIP3, higher gain and better input return loss. Since a filter exists before the LNA in some transceiver systems, poor input return loss will degrade the performance of the filter, and thus impact the total performance of the system. The goal for the input matching is to achieve good return loss and noise figure while maintaining acceptable gain and IIP3.

From Figure 2, the transistor has a  $S^*_{11} = 0.608 \angle 149.6^\circ$ , which is a little far away from  $\Gamma_{opt} = 0.32 \angle -170^\circ$ . This means that if we wish to obtain a good input return loss, the noise figure will be high; if we wish to obtain a good noise figure, the VSWR will be high. The best way to solve this contradiction is to obtain good noise figure and good return loss. This could be implemented by pulling  $S^*_{11}$  close to  $\Gamma_{opt}$  via a feedback network.

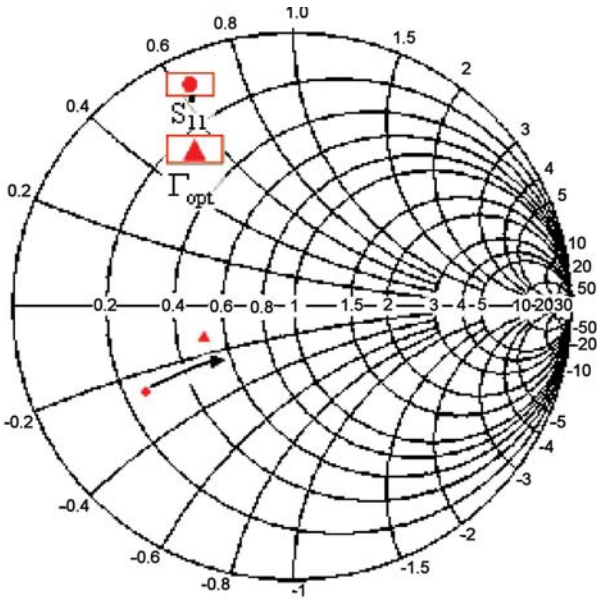


Figure 2. Input and  $\Gamma_{opt}$

### Negative feedback to pull $S^*_{11}$ closer to $\Gamma_{opt}$

According to the theory of H. Nyquist, the noise from any impedance is determined by its resistive component [4], and an ideal loss-less element will not impact the NFmin if it is applied as the feedback network [5].

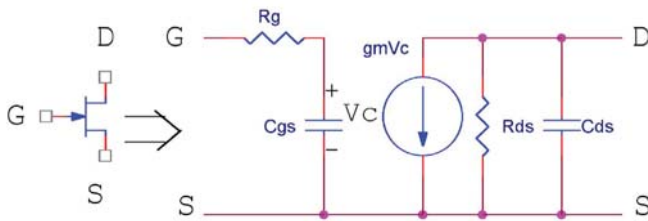


Figure 3. Simplified FET model (reference 6)

In Figure 3,

$$Z_{in} = R_g + \frac{1}{j\omega C_{gs}} \quad (1)$$

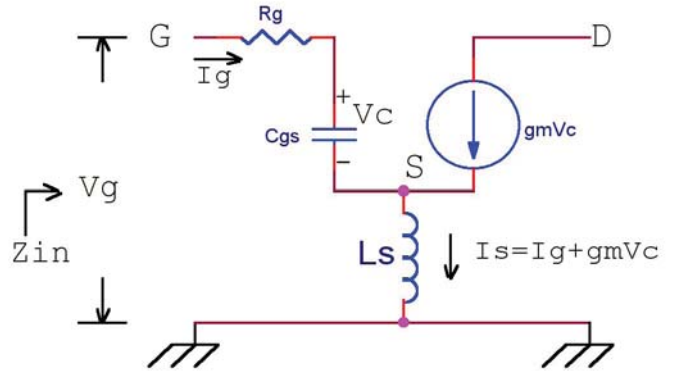


Figure 4. FET model with external source inductance

In Figure 4, by means of adding source inductance  $L_s$  at the FET's source lead, the input voltage can be rewritten as:

$$V_g = I_g \cdot \left( R_g + \frac{1}{j\omega C_{gs}} \right) + (I_g + g_m V_c) \cdot j\omega L_s \quad (2)$$

Since

$$V_c = \frac{I_g}{j\omega C_{gs}} \quad (3)$$

Then  $V_g$  can be expressed as:

$$\begin{aligned} V_g &= I_g \cdot \left( R_g + \frac{1}{j\omega C_{gs}} \right) + \left( I_g + g_m \frac{I_g}{j\omega C_{gs}} \right) \cdot j\omega L_s \\ &= I_g \cdot \left( R_g + \frac{1}{j\omega C_{gs}} + j\omega L_s + \frac{g_m \cdot L_s}{C_{gs}} \right) \end{aligned} \quad (4)$$

Thus the equivalent input impedance is

$$Z'_{in} = \frac{V_g}{I_g} = \left( R_g + j\omega L_s \right) + \left( \frac{1}{j\omega C_{gs}} + \frac{g_m \cdot L_s}{C_{gs}} \right) \quad (5)$$

In equation (5), the term  $\frac{g_m \cdot L_s}{C_{gs}} + j\omega L_s$  is "added"

input impedance introduced by the source inductors, and the added resistive and reactive component both help to pull the  $S^*_{11}$  closer to  $\Gamma_{opt}$ .

Normally, the  $L_s$  should be a small inductor optimized according to the equation. Based on the analysis above, a small microstrip line (width = length = 16 mil) together with a via hole was introduced on both of the source leads to work as a small inductor. According to the measured results, the microstrip lines actually pull the  $S^*_{11}$  closer to

$\Gamma_{opt}$  while not changing the value for  $\Gamma_{opt}$  (stands for the  $NF_{min}$ ). Since the feedback is negative, there is an accompanying decrease in gain with increasing feedback. In this circuit, the gain didn't decrease too much.

### Input Matching Network Design

Since this LNA operates around 3.5 GHz, a high-pass filter is required for input matching. When pulling  $S^*_{11}$  closer to  $\Gamma_{opt} = 0.32 \angle -170^\circ$ , the matching network should also maintain the gain.

In Figure 5, the input conjugate  $S^*_{11}$  is  $0.38 \angle -162^\circ$  after allocating the capacitor, inductor and microstrip lines casually. Figure 6 is the equivalent circuit. According to the measured results, this input matching network will lead to a  $-20$  dB  $S^*_{11}$  and a  $0.82$  dB NF. The measurement results are in line with theoretical analysis and ADS simulation.

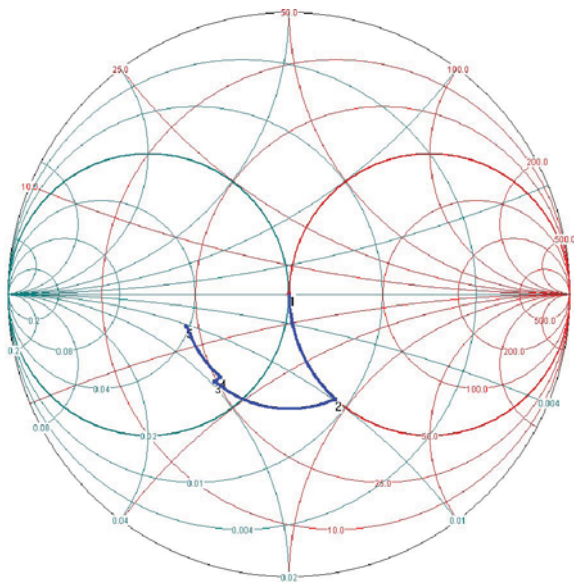


Figure 5. Implementation for input matching

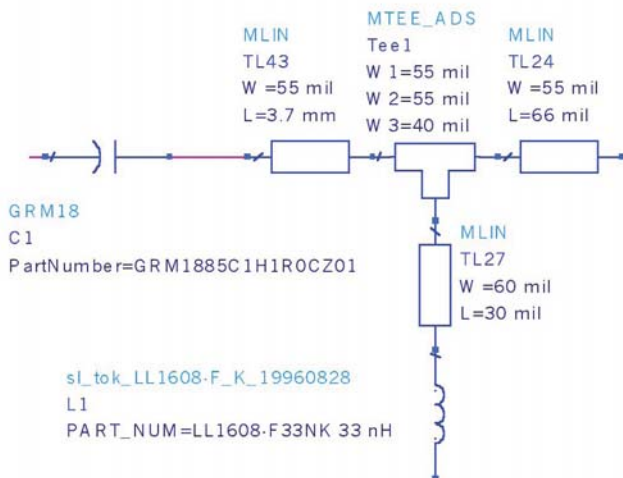


Figure 6. The corresponding circuit for Figure 5

### Passive DC Biasing

Once the RF input matching has been established, the next step is to establish DC biasing. Since the DC biasing conditions are:  $V_{gs} = 0.59$  V,  $V_{ds} = 3$  V,  $I_{ds} = 60$  mA, it's easy to determine the DC biasing for Figure 1:

$$R3 = \frac{V_{dc} - V_{ds}}{I_{ds}} + \frac{3.6 - 3}{60 \times 10^{-3}} = 10 \Omega$$

$$\frac{R1}{R1 + R2} = \frac{V_{gs}}{V_{ds}} = \frac{0.59}{3} = \frac{1}{5}$$

Where:

$V_{dc}$  = the power supply voltage, 3.6 V

$V_{ds}$  = the device drain to source voltage, 3 V

$V_{gs}$  = the device gate to source voltage, 0.59 V

$I_{ds}$  = the device drain to source current, 60 mA

### Determining Device Values

In Figure 6, to achieve low input return loss, low noise figure and high gain, the values for C1, TL43, L1 and TL24 are established according to the analysis of the input matching network design. The width and length of L2 and L3 are determined according to the ADS simulation. The SRF (series resonant frequency) for C5 is selected to be 3.5 GHz to terminate the frequency around 3.5 GHz and thus help improve linearity. C3 and C6 are used as a low frequency bypass to terminate high frequency second order harmonics and thus help improve linearity. Resistor R5 helps terminate low frequencies, and can improve the in-band stability by preventing resonant frequencies between the two bypass capacitors. Table 1 summarizes the bill of material for the LNA board.

Table 1. Component part list for the ATF-54143 WiMAX amplifier

Devices		Vendor's Part Number
C1	1 pF	Murata GRM1885C1H1R0CZ01D
C4	3.6 pF	Murata GRM1885C1H3R6CZ01D
L1	33 nH	Toko LL1608-FH33NJ
L4	10 nH	Toko LL1608-FH10NJ
C2, C5	3.6 pF	Murata GRM1885C1H3R6CZ01D
C3, C6	10 nF	Murata GRM188R71E103KA01D
J1, J2	SMA connectors	E.F. Johnson 142-0701-881
Q1	E-pHEMT	Avago Technologies ATF-54143
R1	300 $\Omega$ chip resistor	
R2	1200 $\Omega$ chip resistor	
R3	10 $\Omega$ chip resistor	
R4	50 $\Omega$ chip resistor	
R5	10 k $\Omega$ chip resistor	
L1, L2	Strap each source pad to the ground pad With 16-mil width and 16-mil length	

### Measured performances of the ATF-54143 at 3.5 GHz

With a drain current of 60 mA, a gain of 12.8 dB as shown in Figure 7 and a noise figure of 0.82 dB (Figure 8) are achieved.

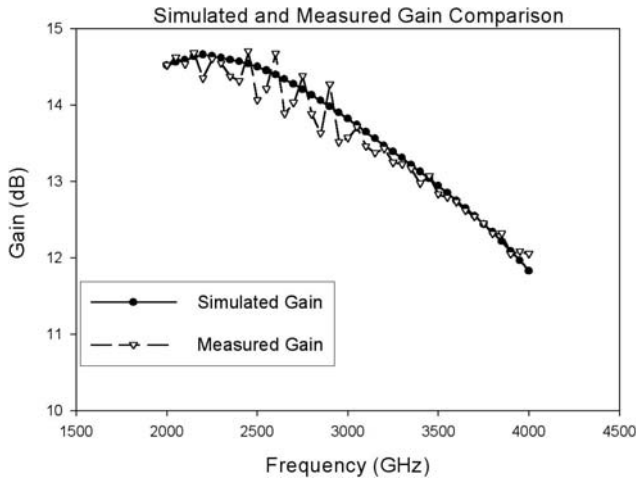


Figure 7. Simulated and measured gain comparison

Figure 9 shows the comparison between the simulated and measured input return loss, both are 20 dB.

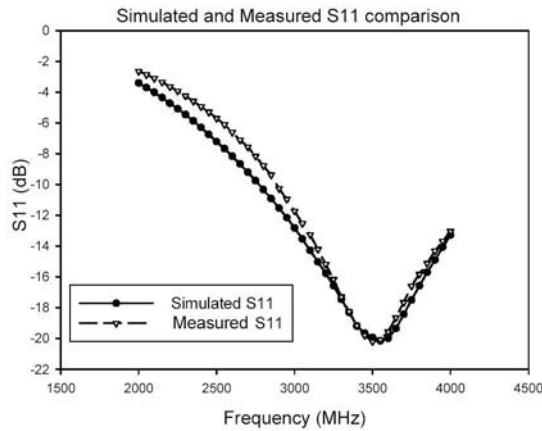


Figure 9. Simulated and measured input return loss comparison

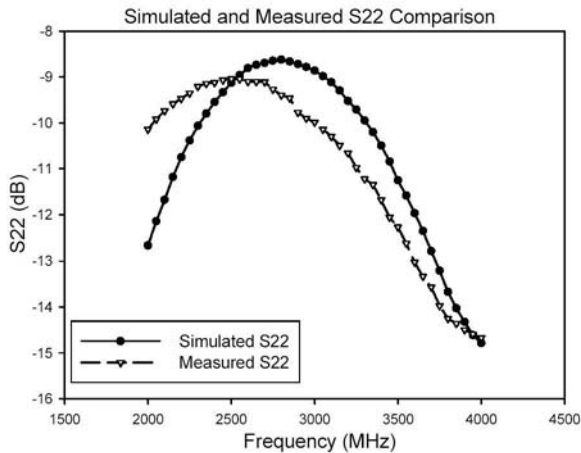


Figure 10. Simulated and Measured Output Return Loss Comparison

The simulated and measured output return loss is shown in Figure 10, both are greater than 11 dB. The response is wide enough to cover the operating frequency range from 3.3 GHz to 3.8 GHz. Figure 11 depicts the comparison for isolation (S12) and Figure 12 is the comparison for OIP3.

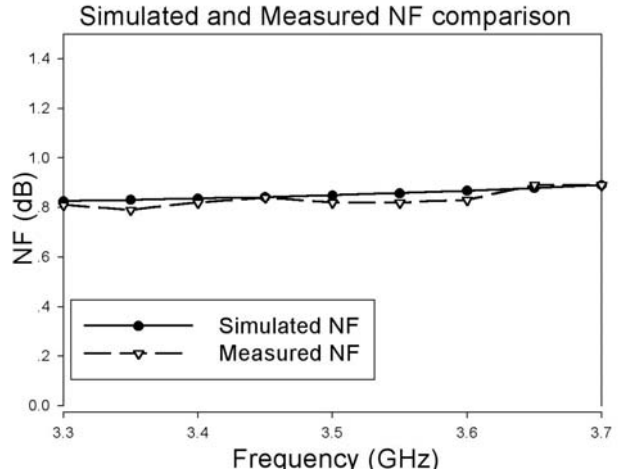
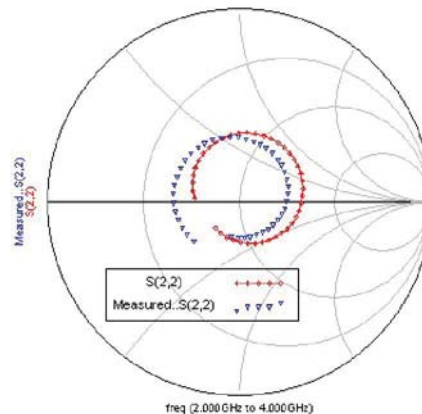
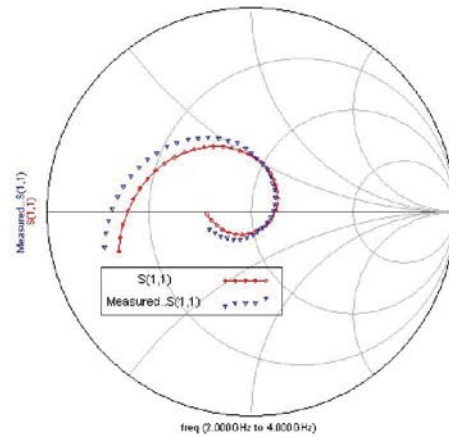


Figure 8. Simulated and measured NF comparison



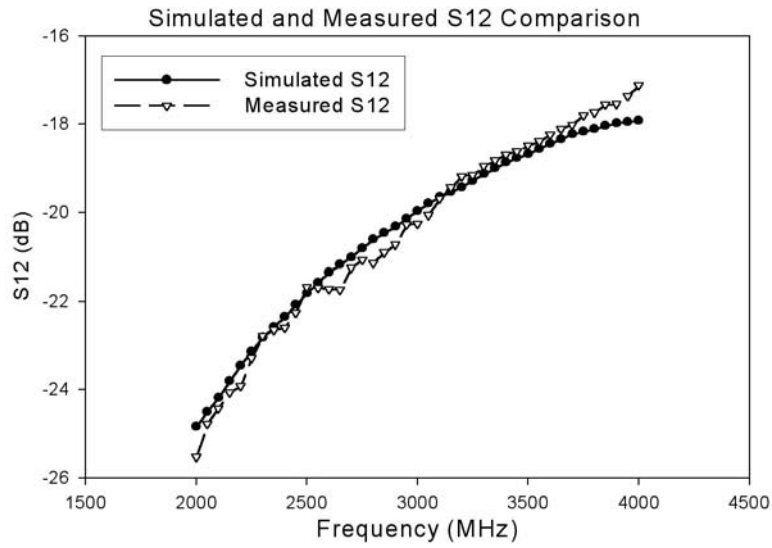


Figure 11. Simulated and measured S12 comparison

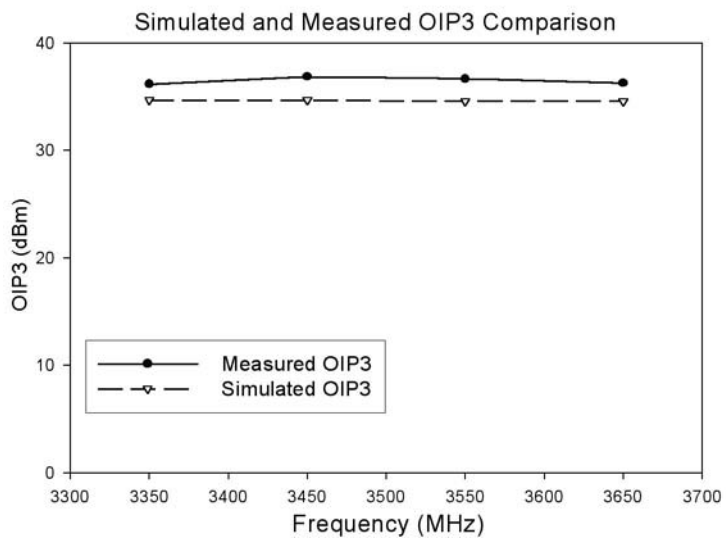


Figure 12. Simulated and measured OIP3 comparison

## Conclusion

Based on theoretical analysis and ADS simulation, this paper demonstrates a 3.3 to 3.8 GHz WiMAX LNA built on FR4 board material. Since it has a high linearity ( $P_{1dB} > +19$  dBm,  $OIP3 > +36$  dBm), this LNA can also be used as a PA driver for radio cards and CPE. The measured RF results verify the feasibility of 3.5 GHz WiMAX designs built on FR4 board. Over the 3.3 GHz to 3.8 GHz operating frequency range, the FR4 board will not significantly impact noise figure and gain.

## Acknowledgements

The author would like to thank Eric Chan, Lim Chin-Leong and Abdullah Asrul-Sani of Avago Technologies Malaysia for their valuable help and comments during the circuit tuning and validation.

## References

- [1] Inder Bahl, Lumped Elements for RF and Microwave Circuits, Artech House, 2003, Chapter 13.
- [2] Data Sheet, RO4000® Series High Frequency Circuit Materials, Rogers Corporation, 2002.
- [3] Data Sheet, Agilent ATF-54143 Low Noise Enhancement Mode Pseudomorphic HEMT in a Surface Mount Plastic Package, Agilent Technologies, Inc., 2003.
- [4] Inder Bahl, Prakash Bhartia, Microwave Solid State Circuit Design, John Wiley & Sons, 1988, Chapter 7.
- [5] J. Engberg and T. Larsen, Noise Theory of Linear and Nonlinear Circuits, John Wiley & Sons, 1995, Chapter 6.
- [6] Stephen A. Maas, Nonlinear microwave and RF circuits, Artech House, 2003, Chapter 8

For product information and a complete list of distributors, please go to our web site: [www.avagotech.com](http://www.avagotech.com)

Avago, Avago Technologies, and the A logo are trademarks of Avago Technologies in the United States and other countries.  
Data subject to change. Copyright © 2005-2010 Avago Technologies. All rights reserved.  
AV02-2418EN - March 25, 2010

**AVAGO**  
TECHNOLOGIES